NeuroImage: Clinical 25 (2020) 102142

Contents lists available at ScienceDirect

NeuroImage: Clinical

journal homepage: www.elsevier.com/locate/ynicl

Neural correlates of rumination in major depressive disorder: A brain network analysis

Yael Jacob[a,*], Laurel S Morris[b], Kuang-Han Huang[a], Molly Schneider[b], Sarah Rutter[b], Gaurav Verma[a], James W Murrough[b,c,1], Priti Balchandani[a,1]

[a] BioMedical Engineering Imaging Institute, Icahn School of Medicine at Mount Sinai, New York, NY, United States
[b] Depression and Anxiety Center for Discovery and Treatment, Department of Psychiatry, Icahn School of Medicine at Mount Sinai, New York, NY, United States
[c] Department of Neuroscience, Icahn School of Medicine at Mount Sinai, New York, NY, United States

ARTICLE INFO

Keywords:
Default mode network
Depression
Entropy
Graph Theory
High-field MRI
Precuneus

ABSTRACT

Patients with major depressive disorder (MDD) exhibit higher levels of rumination, i.e., repetitive thinking patterns and exaggerated focus on negative states. Rumination is known to be associated with the cortical midline structures / default mode network (DMN) region activity, although the brain network topological organization underlying rumination remains unclear. Implementing a graph theoretical analysis based on ultra-high field 7-Tesla functional MRI data, we tested whether whole brain network connectivity hierarchies during resting state are associated with rumination in a dimensional manner across 20 patients with MDD and 20 healthy controls. Applying this data-driven approach we found a significant correlation between rumination tendency and connectivity strength degree of the right precuneus, a key node of the DMN. In order to interrogate this region further, we then applied the Dependency Network Analysis ($D_{EP}NA$), a recently developed method used to quantify the connectivity influence of network nodes. This revealed that rumination was associated with lower connectivity influence of the left medial orbito-frontal cortex (MOFC) cortex on the right precuneus. Lastly, we used an information theory entropy measure that quantifies the cohesion of a network's correlation matrix. We show that subjects with higher rumination scores exhibit higher entropy levels within the DMN i.e. decreased overall connectivity within the DMN. These results emphasize the general DMN involvement during self-reflective processing related to maladaptive rumination in MDD. This work specifically highlights the impact of the MOFC on the precuneus, which might serve as a target for clinical neuromodulation treatment.

1. Introduction

Rumination is conceptualized as repetitive thinking and focus on one's distress and negative mood states with a high self-critical nature (Nolen-Hoeksema et al., 1993). Patients with major depressive disorder (MDD) exhibit increased levels of rumination (Nolen-Hoeksema et al., 2008) which increases the risk of depressive relapse in remitted patients (Roberts et al., 1998). However, the neural mechanisms that underlie ruminative processes are still unclear. Unveiling these underlying biomechanisms could potentially shed more light on MDD mechanisms, serve future therapy and improve well-being in depressed individuals, as well as other patient populations characterization by pathological ruminative processes. This is in accordance with the growing interest in utilizing the Research Domain Criteria (RDoC) (Sanislow et al., 2010) to classify mental disorders based on dimensions of observable behavior and neurobiological measures.

Rumination is known to involve a wide range of affective and cognitive subprocesses such as attention, self-referential processing, and recall of autobiographical memories (Cooney et al., 2010) which manifests in the activation of different brain regions. Importantly, there is a growing literature that characterizing neural network features during resting-state functional MRI (rsfMRI), a task-negative state during which ruminative processes can predominate (Gusnard et al., 2001; Hamilton et al., 2011). Subsequently, rumination has been associated with aberrant activity and connectivity of various regions such as the medial prefrontal cortex (mPFC), anterior cingulate cortex (ACC), posterior cingulate cortex (PCC), precuneus primarily, as well as the insula, temporal pole, hippocampus, and amygdala (Gusnard et al., 2001; Fossati et al., 2003; Ochsner and Gross, 2005; van der Meer et al., 2010; Nejad et al., 2013; Northoff et al., 2006). The mPFC, ACC, PCC

* Corresponding author.
E-mail address: yael.jacob@mssm.edu (Y. Jacob).
[1] Equal contributions.

https://doi.org/10.1016/j.nicl.2019.102142
Received 11 October 2019; Received in revised form 11 December 2019; Accepted 21 December 2019
Available online 23 December 2019

Table 1
Demographic and clinical characteristics

	MDD (n = 20)	HC (n = 20)	t (df)	p
Male (frequency, %)	10, 50%	14, 70%	1.29	0.2
Age, years (mean ± SD)	33.35 ± 9.28	41.45 ± 10.97	−2.3 (38)	0.02*
Age at first episode (mean ± SD)	19.74 ± 9.96	–	–	–
Years since first episode (mean ± SD)	13.55 ± 6.32	–	–	–
Number of episodes (mean ± SD)	7.37 ± 12.20	–	–	–
Duration of current episode, months (mean ± SD)	54.26 ± 70.77	–	–	–
Recurrent MDD (frequency, %)	14, 70%	–	–	–
Current PPD (frequency, %)	13, 65%	–	–	–
MADRS	29.95 ± 6.22	0.65 ± 1.26	2.02 (38)	2.86E−22*
RRS total	57.05 ± 12.78	29.65 ± 8.47	7.99 (38)	1.17E−09*
RRS – depression	32.60 ± 7.29	15.20 ± 3.61	9.57 (38)	1.14E−11*
RRS – brooding	12.60 ± 4.02	7.10 ± 2.31	5.30 (38)	5.12E−06*
RRS – reflection	11.85 ± 3.41	7.35 ± 3.34	4.22 (38)	1.48E−04*

MDD major depressive disorder, *HC* healthy controls, *PPD* Persistent Depressive Disorder, *MADRS* Montgomery Åsberg Depression Rating Scale, *RSS* Ruminative Response Scale.
* $p < 0.05$ for MDD group compared to healthy control group

and precuneus are key nodes of the dominant intrinsic default mode network (DMN) (Northoff and Bermpohl, 2004; Fox et al., 2005; Raichle, 2010; Raichle et al., 2001), the primary task-negative neural network involved in self-referential processing (Fox et al., 2005; Qin and Northoff, 2011; Gusnard et al., 2001), autobiographical memory (Spreng et al., 2009; Philippi et al., 2014) and social cognition processes (Mars et al., 2012; Schilbach et al., 2008). Furthermore, maladaptive rumination in depression is thought to involve excessive DMN activity and a blunted ability to reduce DMN activity in response to external cues (Sheline et al., 2009). As such, neural network features during the resting-state provide a critical substrate for understanding ruminative features, relevant to depression.

However, previous rsfMRI studies investigating the resting-state neural networks underlying rumination have shown inconsistent results (Mulders et al., 2015), likely related to their hypothesis-driven designs. Two seed-based functional connectivity studies have shown that rumination is associated with higher connectivity between a PCC seed region and subgenual ACC, and lower connectivity between a subgenual ACC seed region and the medial frontal cortex (Cooney et al., 2010; Berman et al., 2011). However, since these studies are hypothesis-driven and focus on the co-activation of one network node at a time, they lose important information relating to the entire neural network, its interactions and its topology. Therefore, there is a need for a more data-driven approach to the identification of underlying functional network motifs embedded in the rich, whole brain rsfMRI data.

The mathematical field of graph theory recently emerged as a tool for characterizing brain network features that can distinguish between processes, as well as between healthy and pathological states (Bassett et al., 2008; Bullmore and Sporns, 2009; Sporns, 2010). The functional brain network graph is composed of nodes, representing regions of interest (ROIs), and edges, representing connections. Global topological architectures of the graph (e.g., characteristic path length, clustering coefficient, and global efficiency) measure the overall information integration or segregation of the network, whereas local nodal features (e.g., node strength, betweenness centrality and local efficiency) are used to depict the network regions' hierarchy and identify hubs that are critical for efficient information flow (Sporns, 2010). Another recent advancement in the mathematical approach to understanding neural networks is the development of the Dependency Network Analysis ($D_{EP}NA$) (Jacob et al., 2018; Jacob et al., 2018; Jacob et al., 2019; Jacob et al., 2018; Jacob et al., 2016). This analysis quantifies the influence of a node over the connectivity of other nodes, offering a new computational method for measuring the direction of influence among neural network nodes, thereby facilitating the characterization of critical network pathways that underlie specific cognitive processes. While the classical graph theory approach has already successfully demonstrated aberrant topological organization of the connectome of MDD patients (Gong and He, 2015), the application of these novel data-driven approaches to understanding rumination has been largely overlooked.

Here, we examined how whole brain neural network topological features relate to rumination tendencies using ultra-high field 7-T MRI. Our recently developed 7-T functional MRI scanning protocol with echo-time (TE) dependent physiological denoising method allows for significantly improved signal power detection and temporal SNR compared to 3-T MRI (Morris et al., 2019), features that are critical for graph theory connectivity analyses. Utilizing these advantages, data-driven graph theory analysis was implemented to test whether whole brain global network features or local network hierarchies during rsfMRI are associated with rumination in MDD and HC. We also applied the Dependency Network Analysis ($D_{EP}NA$) (Jacob et al., 2018a,b,c, 2019, 2016), a recently developed graph theory method to quantify network node importance according to its partial correlation influence. $D_{EP}NA$ does not rely on temporal resolution, an advantage compared to Granger causality (Goebel et al., 2003). Also, as opposed to dynamic causal modeling (DCM) (Friston et al., 2003), $D_{EP}NA$ does not require any specific a-priori direction of influence models, which allows the examination of a large set of regions in a data-driven manner. Lastly, in order to specifically test the DMN connectivity in relation to rumination tendency we used an entropy measure to quantify the cohesion of the DMN network. Entropy has been used in statistics and information theory to measure the information content of signals (Shannon, 1949) and can quantify the deviation in connectivity metrics from a uniform matrix (Alter et al., 2000). This idea has been applied in the context of biological systems (Varshavsky et al., 2007), economic systems (Shapira et al., 2009) and recently, neural systems (Jacob et al., 2010). Entropy provides a measure of DMN connectivity integration and its relation to rumination tendencies.

2. Methods and materials

2.1. Participants

Participants included 20 MDD patients (10 females) and 20 (6 females) HC. The demographic and clinical variables are presented in Table 1. All subjects were recruited at the Depression and Anxiety Center for Discovery and Treatment (DAC) at Icahn School of Medicine at Mount Sinai. All participants underwent the Structured Clinical Interview for DSM-V Axis Disorders (SCID-V) by a trained rater to determine any current or lifetime psychiatric disorder (First et al., 2015). Subjects were excluded if they had an unstable medical illness, history of neurological disease, history of schizophrenia or other psychotic

disorder, neurodevelopmental/ neurocognitive disorder, substance use disorder within the past 2 years, any contraindications to MRI, or positive urine toxicology on the day of scan. HC subjects were free from any current or lifetime psychiatric disorder. All participants were free of antidepressant medication or other psychotropic medication for at least 4 weeks (8 weeks for fluoxetine) prior to data collection. Inclusion criteria for MDD subjects included having MDD as their primary presenting problem and being in a current major depressive episode. In all subjects, depressive symptom severity was measured by a clinician with the Montgomery–Åsberg Depression Rating Scale (MADRS) (Montgomery and Asberg, 1979) and the rumination tendency was assessed by the Ruminative Responses Scale (RRS) (Treynor et al., 2003). All data was collected under Institutional Review Board (IRB) approved written informed consent and participants were compensated for their time.

2.2. MRI data acquisition

Data were acquired on a Siemens Magnetom 7T MRI scanner (Erlangen, Germany) with a 32-channel head coil (Nova Medical, Wilmington, MA). Each imaging session included acquisition of anatomical scan using a twice magnetization-prepared rapid gradient echo (MP2RAGE) sequence for improved T1-weighted contrast and spatial resolution (Marques et al., 2010), with the following parameters: 0.7 mm isotropic resolution, 60 slices, TR/TE = 6000/3.62 ms, field of view = 240 × 320, bandwidth = 300.

The resting-state fMRI scan was 10 min long and involved acquisition of multi-echo multi-band time course EPI using the following parameters: 2.5 mm isotropic resolution, 50 slices, TR/TE's = 1850/8.5, 23.17, 37.84, 52.51, MB = 2, iPAT acceleration factor = 3, 300 frames, flip = 70, field of view = 640 × 640, pixel bandwidth = 1786. The subjects were instructed to remain awake and keep their eyes open during the scan.

2.3. MRI data preprocessing

Functional images were processed using the multi-echo independent component analysis (ME-ICA) (Kundu et al., 2012) implemented in the AFNI meica.py toolbox (Cox, 1996). The ME-ICA preprocessing pipeline exploits the property that BOLD percent signal change is linearly dependent on TE, a consequence of T2* decay (Kundu et al., 2012, 2017). ME-ICA decomposes multi-echo functional MRI data into independent components, and computes the TE dependence of the BOLD signal for each component and then categorized as BOLD or non-BOLD. Removing non-BOLD components allows for robust denoising of the data for motion, physiological and scanner artefacts (Kundu et al., 2012, 2017). Morris et al. (2019) recently demonstrated the improved signal power across the brain with ultra-high field 7 T fMRI compared to 3 T that was further increased by applying the ME-ICA denoising pipeline.

Each subjects anatomical T1 brain image was segmented into the Desikan-Killiany Atlas (Desikan et al., 2006) applied in FreeSurfer 6.0. The segmentation resulted in 84 regions of interest (ROIs) and their volumes in the subject's native space (Fig. 1A). The structural image and parcellations were then co-registered to the functional data using SPM12 and resampled to have the same voxel resolution using AFNI's 3dresample (Cox, 1996). Then the averaged BOLD signal (time series) was extracted for each ROI mask image and each subject using AFNI's 3dNetCorr (Cox, 1996).

2.4. Graph theory analysis

Each of the 84 anatomical segmented ROIs represents a node in the graph (Fig. 1A). In order to define the network edges, we calculated the partial correlation coefficients between the regional mean time-series of all pairwise regions (excluding the effects of all other regions) (Fig. 1C). To ensure that the number of nodes and connections are matched across participants, we used a sparsity threshold S, which retains S% of the top connections for each subject (Korgaonkar et al., 2014) (Fig. 1D).

Using the Brain Connectivity Toolbox (Rubinov and Sporns, 2010), we examined common global network properties; 1) *characteristic path length*, λ, which is the average shortest path length in the network; 2) *clustering coefficient*, γ, which quantifies the probability that two nodes connected to a given node are also connected with each other; and 3) *efficiency* (Eglob), which is the average inverse shortest path length in the network. As well as local nodal centrality features; 1) *node strength,* which is the sum of weights of links connected to the node (Fig. 1E); 2) *betweenness centrality*, which is a measure of the number of shortest paths that traverse a given node; and 3) *local efficiency*, which is the global efficiency computed on a given node neighbors.

We examined the network global and local features across a range of thresholds ($10\% < S < 30\%$ in steps of 1%) (Korgaonkar et al., 2014). We then calculated the area under the curve for each network feature, which provides a summarized measure independent of single threshold selection (Korgaonkar et al., 2014) (Fig. 1F).

2.5. Dependency network analysis ($D_{EP}NA$)

To further explore the information flow of the significant network regions that were found using the local network features we applied the $D_{EP}NA$. $D_{EP}NA$ is a graph-theory method to quantify networks' node importance according to its influence (Jacob et al., 2018a,c, 2016). The steps needed to calculate the network's regions influence are described in Fig. 2 and in (Jacob et al., 2016). First, the pairwise ROI–ROI connectivity matrix was calculated using Pearson correlations and normalized using a Fisher r-to-Z transformation. We then define the influence of node j on the pair of elements i and k as the difference between the correlation and the partial correlation, given by the following equation:

$$d(i,\, k|j) \equiv C(i,\, k) - PC(i,\, k|j)$$
$$PC(i,\, k|j) = \frac{C(i,k) - C(i,j)C(k,j)}{\sqrt{[1 - C^2(i,j)][1 - C^2(k,j)]}} \quad (1)$$

This quantity is large only when a significant fraction of the correlation between nodes i and k can be explained in terms of node j (Fig. 2A). We then calculate the partial correlation effect for each ROI (i.e. node) on all other pairwise correlations in the network. We define the total influence of node j on node i, D(i,j) as the average influence of node j on the correlations C(i,k), over all nodes k (Fig. 2B), given by:

$$D(i,\, j) = \frac{1}{N-1} \sum_{k \neq j}^{N-1} d(i,\, k|j) \quad (2)$$

The node dependencies define a dependency matrix D, whose (i,j) element is the influence of node j on node i. It is important to note that the dependency matrix is nonsymmetrical since the influence of node j on node i is not equal to the influence of node i on node j.

All pairwise ROIs with dependency elements D that are significantly correlated with the RRS score at the $p < 0.05$ level FDR corrected are plotted as graph edges (Fig. 2C). This allows for a simple graph visualization of the influences significantly related to rumination.

2.6. Calculation of network entropy

In order to quantify the total DMN network cohesion (i.e. network integration), we applied an information theory quantity called *Shannon's entropy* (Jacob et al., 2012). This measure quantifies the amount of latent information contained in each condition's correlation matrix. The DMN comprised 8 bilateral brain regions (Kabbara et al., 2017); medial orbito-frontal cortex (MOFC), PCC, precuneus, isthmus-cingulate, rostral anterior cingulate cortex, lateral orbito-frontal, inferior parietal and parahippocampal. Pearson correlations between the time courses of the DMN network's ROIs were used to calculate the ROI-

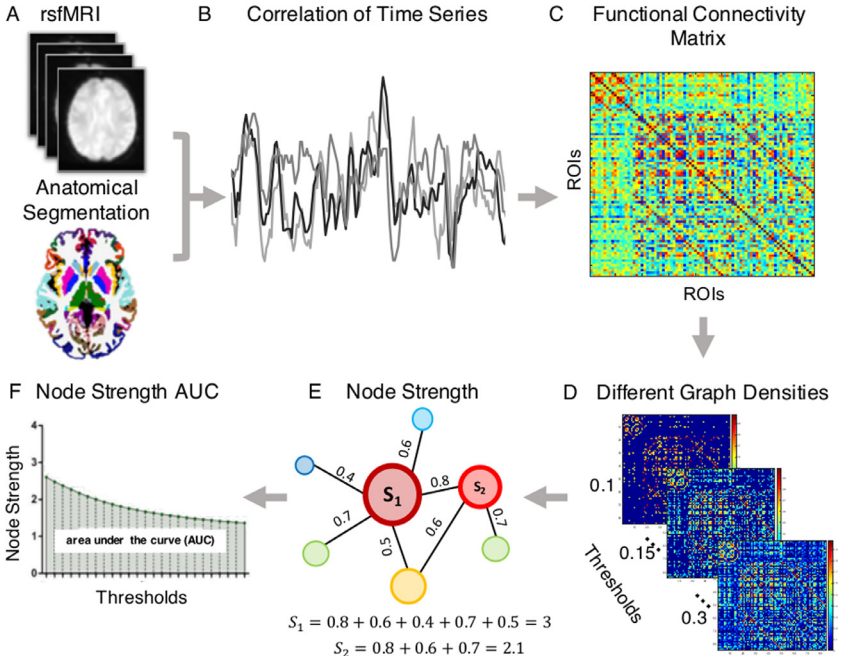

Fig. 1. Functional network graph theory analysis. (A) Each subjects anatomical brain image was segmented into 84 regions. (B) We then extracted the averaged fMRI time-course per region. (C) To define network edges, we calculated the partial correlation coefficients between all pairwise regions. (D) A threshold of the top connections for each network was applied across a range from 0.1 to 0.3. (E) We then examined the network property of node strength which is the sum of weights of links connected to the node. (F) The area under the curve for each threshold was used to provide a measure independent of single threshold selection.

ROI correlation matrices for each subject.

We then calculated the eigenvalue entropy for each subject defined by (Eq. 5.3),

$$S = -\frac{1}{\log(N)} \sum_{i=1}^{N} \Omega(i)\log[\Omega(i)] \tag{3}$$

N is the number of regions in the network, and $\lambda(i)$ denotes the correlation matrix eigenvalues. S ranges from 0 to 1. Note that 1/log(N) is a normalization factor ensuring that S reaches its maximum ($S = 1$) for a uniform eigenvalue distribution (i.e. random correlations matrix).

2.7. Statistical analysis

As the MDD exhibit significantly higher levels of rumination compared to HC ($t = 7.99(38)$, $p < 1.2E-09$), we tested the effect separately for each group to control for group effect. For each group, we conducted Pearson correlations to assess the association between the graph theory network features and the subjective rumination scores. Partial correlation was used to control for age, gender and region volume as covariates. All results were corrected for multiple comparisons using false discovery rate (FDR) (Benjamini and Hochberg, 1995) correction ($q < 0.05$) where global measures were corrected for the number of global network measures [i.e. 3], and local measures were corrected for number of nodes [i.e. 84].

To further explore the network ROIs that were depicted using the local network features we applied the $D_{EP}NA$. The ROIs $D_{EP}NA$ dependency elements D were correlated to the RRS scores using Pearson correlations. Partial correlations were used to control for age, gender and region volume as covariates. The correlations results were then corrected for multiple comparisons using FDR, where each direction of influences (i.e. influences on, or influenced by all other regions) were corrected for the number of regions minus the ROI [i.e. 83].

For the entropy analysis, for each group we calculated the correlation between each subjects' RRS scores and their DMN entropy measure using Pearson partial correlation controlling for age and gender.

In order to account for clinical specificity, for all results, comparison between the MDD and HC correlation coefficients were conducted using z-fisher transformation. According to statistical power analysis using Monte Carlo simulation (Gelman and Hill, 2006) (see details in Appendix 1), in order to achieve a statistical power of 80% given a sample size of 20 subjects the magnitude of the effect needed to be as high as $r = 0.53$ (Figure A1). Finally, to compare the network features between the MDD and HC we conducted a between-group t-test for each global feature and each region's local feature (see details in Appendix 1).

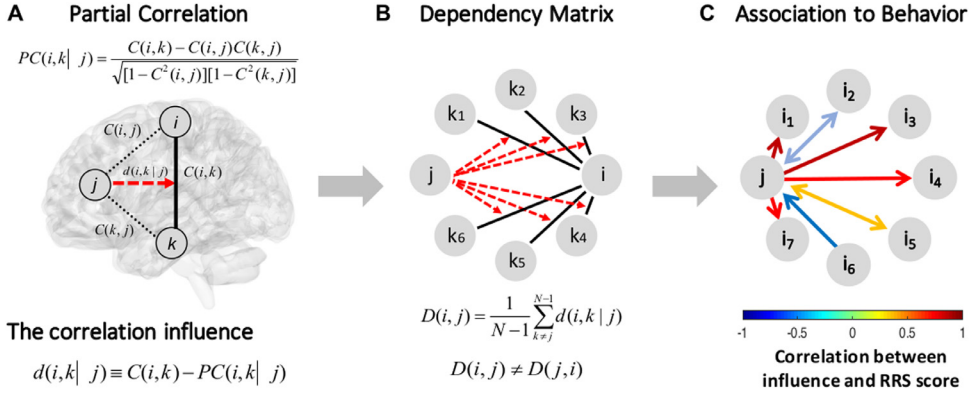

Fig. 2. Dependency Network Analysis. (A) The correlation influence of node j on the pair of nodes i and k is defined as the difference between their correlation C(i,k) and their partial correlation with respect to the node j - PC(i,k| j). The partial correlation coefficient is a statistical measure indicating how a third variable affects the correlation between two other variables. Thus, the correlation influence measure d is large only when a significant fraction of the correlation between nodes i and k can be explained by the influence of node j. (B) Next, we calculate the partial correlation effect for each ROI on all other pairwise correlations in the network. We define the total influence of node j on node i, D(i,j) as the average influence of node j on the correlations C(i,k), over all nodes k (in this study the whole brain network consisted of 84 nodes). The node dependencies define a dependency matrix D, whose (i,j) element is the influence of node j on node i. (C) All pairwise ROIs with dependency elements D that are significantly correlated to the RRS score are plotted as edges. Each edge is color-coded according to the correlation coefficient. The arrows represent the direction of influence.

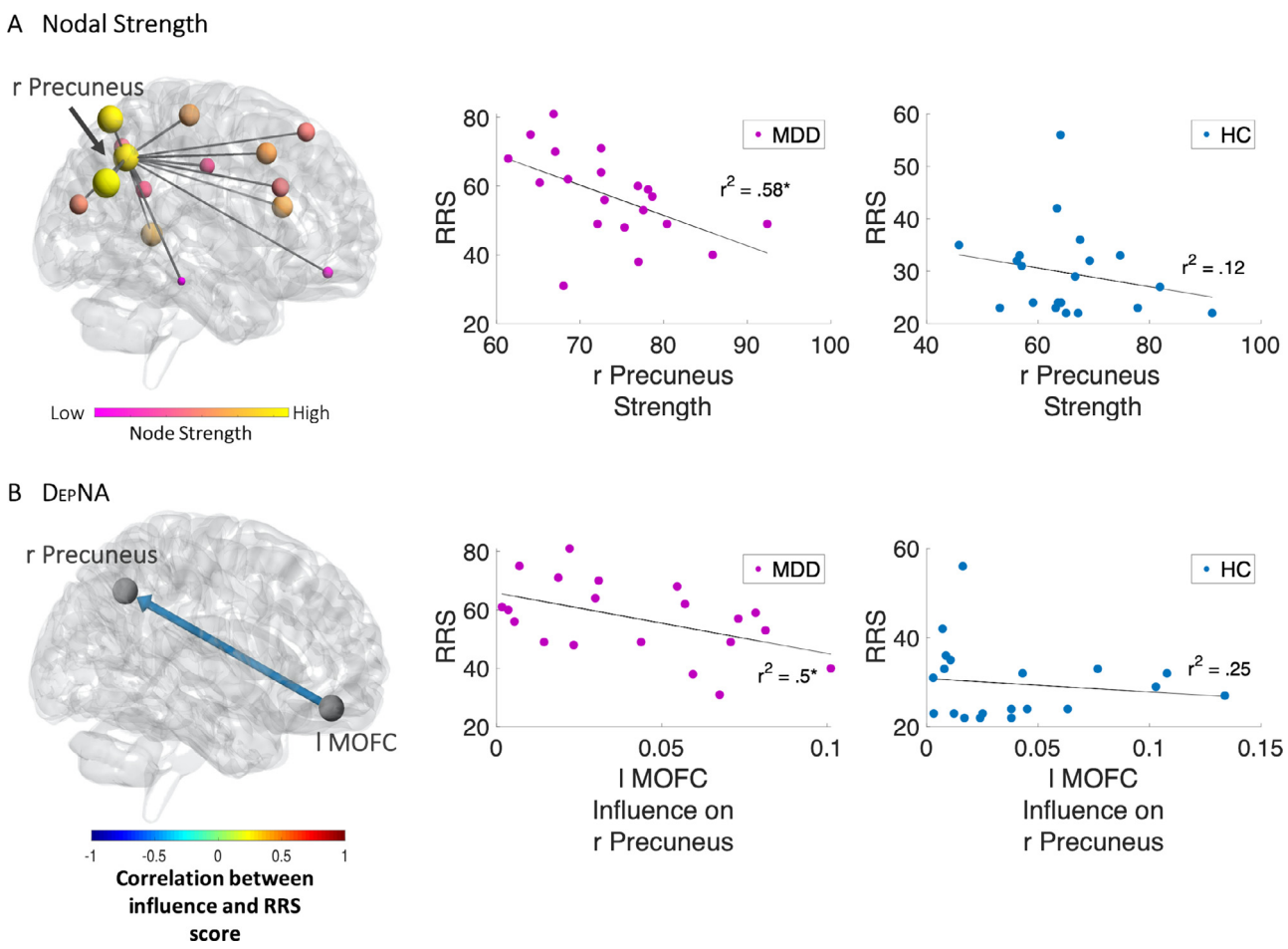

Fig. 3. Rumination correlates with graph features. (A) Within the MDD group, the right precuneus connectivity strength exhibited statistically significant negative correlation with the subjective rumination scores. The lower the region's strength the less its signal was correlated to the rest of the brain regions. For visualization purposes, the brain image illustrates only the averaged right precuneus connectivity among the MDD group. (B) Additional exploration applying the DEPNA, we found that within the MDD group, greater rumination tendency was associated with decreased influence of the left MOFC on the right precuneus. *$p < 0.05$ FDR corrected.

3. Results

To test our hypothesis regarding the relation between network topology and rumination tendencies, we investigated the correlation between the global (e.g., characteristic path length, global efficiency and clustering coefficient) and local (e.g., node strength, betweenness centrality and local efficiency) whole brain network features and total rumination scores from the RRS (Treynor et al., 2003) using FDR correction for multiple comparisons. For both MDD and HC groups none of the topological global features showed significant association with rumination scores (i.e. total rumination and subscales) after correcting for multiple comparisons (see Table A1 in Appendix 1). However, in the local network analysis, the right precuneus node strength was negatively correlated with the total rumination scores in MDD subjects ($r = -0.76$, $p < 0.0003$, $qFDR < 0.05$) (Fig. 3A). In other words, higher subjective reported tendency to ruminate was associated with lower right precuneus connectivity to the rest of the brain network. Also, we note that the homologues left precuneus was also negatively correlated with the total rumination scores in MDD subjects ($r = -0.54$, $p < 0.03$), however did not withstand FDR correction.

Among the HC group, none of the local network features was found to be significantly associated with the rumination scores after correcting for multiple comparisons. Specifically, for the right precuneus strength, we found a negative trend with the total rumination score ($r = -0.35$, p = 0.18). Comparison of the correlation coefficients between the MDD and HC groups using z-fisher transformation was non-significant ($z = 1.84$, $p = 0.07$) indicating that although this effect was not found within the HC group it does not indicate clinical specificity for MDD.

Further exploration of the information flow to and from the precuneus, applying the DEPNA method, revealed that greater rumination tendency was associated with its decreased influence by the left medial orbito-frontal cortex (MOFC) ($r = -0.71$, $p < 0.002$, $qFDR < 0.05$ seed level correction) in MDD (Fig. 3B). This result indicates that patients with higher tendency to ruminate exhibit an aberrant communication between two major DMN regions; the MOFC and precuneus. In addition, this pathway of left MOFC influence on the right precuneus was also found to be correlated with total RRS among the HC subjects ($r = -0.50$, $p < 0.04$, uncorrected). Comparison of the correlation coefficients between the MDD and HC groups using z-fisher transformation was non-significant ($z = 0.96$, $p = 0.32$) denoting no clinical specificity.

Finally, in order to examine whether DMN cohesion was associated with rumination, we calculated the DMN entropy measure. This analysis revealed that higher rumination scores were associated with higher DMN entropy levels both among MDD and HC ($r = 0.47$, $p < 0.04$, and $r = 0.50$, $p < 0.04$ respectively) (Fig. 4). This indicates that the DMN is less cohesive or integrated among subjects with high levels of rumination. Comparison of the correlation coefficients between the MDD and HC groups was non-significant ($z = -0.11$, $p = 0.9$) indicating no clinical specificity.

We note that all the result were controlled for age and gender and

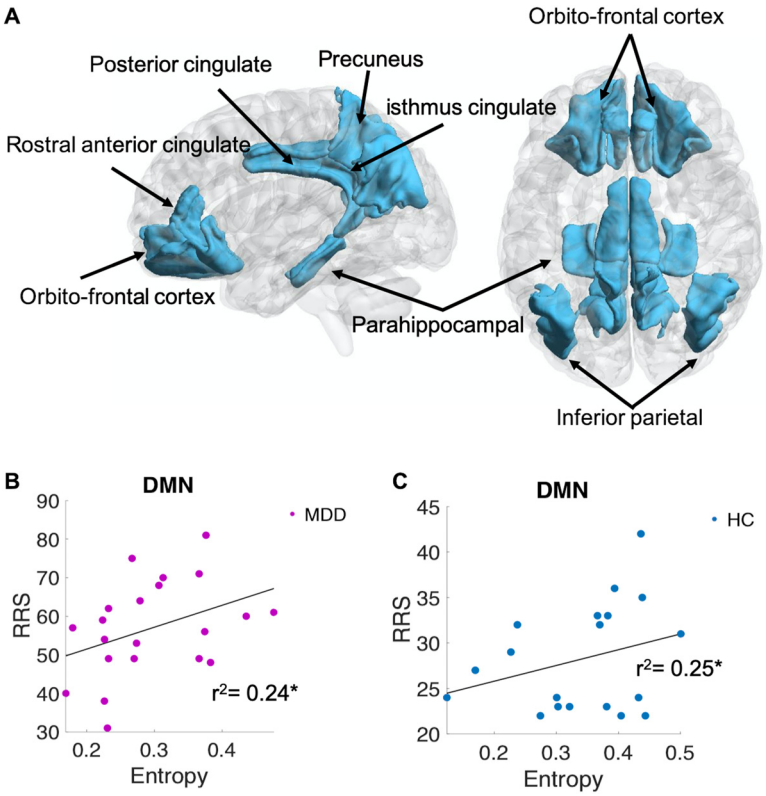

Fig. 4. DMN entropy measure association with rumination. (A) Illustration of the DMN related regions. Specific investigation of the DMN connectivity revealed that increased entropy, which indicates reduced connectivity in the network, was associated with the total rumination scores both among the MDD (B) and HC (C). The DMN comprised of 7 bilateral ROIs; MOFC, PCC, precuneus, isthmuscingulate, rostral anterior cingulate cortex, lateral orbito-frontal and parahippocampal. *$p < 0.05$

they did not show a significant effect on the network features measures.

Between-group comparison of the global graph theory network features, the $D_{EP}NA$ features and entropy showed no differences between MDD patients as compared to controls during resting state (see Appendix 1). Some local graph theory network node features were different between groups (see Appendix 1), replicating previous studies (Gong and He, 2015; Zhang et al., 2011). A specific, non-corrected, investigation of the r precuneus node strength showed significantly lower precuneus connectivity in MDD compared to HC ($t = 2.8$, $p < 0.009$, non-corrected), a finding that did not survive FDR correction.

4. Discussion

Using a data-driven graph-theory approach with high-field 7-T functional MRI data, we investigated the relationship between the topological architecture of functional brain networks and subjective rumination scores in MDD patients and HC. Global network features of characteristic path length, efficiency and clustering coefficient were not predictive of rumination levels. However, data-driven analysis of the network hierarchy according to node strength showed that reduced strength of the right precuneus, which is one of the main DMN regions, was associated with higher maladaptive rumination levels among MDD patients. In addition, patients with higher rumination tendency exhibited decreased influence of another DMN related region, the left MOFC, on the right precuneus as depicted by the recently described $D_{EP}NA$ method (Jacob et al., 2016). Finally, specific investigation of intrinsic DMN connectivity, quantified by the network's entropy, revealed that both healthy and depressed patients with higher rumination scores exhibited decreased overall connectivity within the DMN. Together this multi-level and complementary data-driven analysis indicates reduced cohesion within the DMN, and a specific disruption within a DMN pathway (from the MOFC to the precuneus), which underlies ruminative thought patterns.

The precuneus is one of the major hubs in the brain with dense structural connectivity (Hagmann et al., 2008; Gong et al., 2008; Iturria-Medina et al., 2008). It is also highly metabolically active during rest (Gusnard et al., 2001; Raichle et al., 2001; Greicius et al., 2003) and known to be involved in highly integrated tasks, including self-referential processing, visuo-spatial imagery and autobiographical memory (Cavanna and Trimble, 2006). Interestingly, the precuneus is deactivated during anesthesia (Alkire et al., 2008), sleep (Maquet et al., 1997; Andersson et al., 1998), hypnosis (Rainville et al., 1999) and in different subliminal processes (Kjaer et al., 2001), and is hypothesized to be related to self-consciousness (Bullmore and Sporns, 2009; Cavanna, 2007). Here, we found the precuneus to exhibit decreased centrality (as measured by the node strength) in the whole-brain functional network as patients exhibit higher rumination levels. This result is somewhat contrary to the supposition that a main function of the precuneus concerns self-related processes. One possible explanation for this could be that the precuneus exhibits hyper-activity resulting in an impaired ability to synchronize with the rest of the network, resulting in apparent reduced connectivity. This is in line with a recent study by Dutta et al. (2019) which found the precuneus to be dissociated from the DMN in MDD compared to HC, which was related to greater rumination scores. They further show that after treatment with citalopram, the precuneus integrated back into the DMN. Another study also found decreased connectivity of the PCC/precuneus to the DMN in MDD patients compared to HC (Zhu et al., 2012). In addition, converging evidence indicate that the precuneus is functionally divided into an anterior region, involved in self-referential mental imagery strategies, and a posterior region, involved in episodic memory retrieval (Cavanna and Trimble, 2006). Rumination is, however, a mechanism that can incorporate both self-referential mental imagery strategies and overgeneral autobiographical memory recall. Overall, our results provide additional evidence that the precuneus, and specifically its decreased connectivity to the entire brain, is associated with maladaptive rumination tendencies.

Additionally, the network perspective as captured by the $D_{EP}NA$ method here, demonstrates that influence hierarchies between regions

rather than activity or co-activation may reflect psychological trait at the individual level. Our findings attribute a less active role of the MOFC in shaping the precuneus network connectivity as subject exhibit higher rumination scores. Generally, mPFC regions such as the MOFC have been shown to have reduced functional connectivity among MDD patients (Murrough et al., 2016). In particular our result is also in accordance with intracranial recording and EEG/MEG studies showing that MOFC activity precedes precuneus/PCC responses (Kawasaki et al., 2001). There are no known direct anatomical structural connections between the OFC and the precuneus in humans. Nevertheless, functional connectivity does not require direct anatomical connections, it could be a result of an indirect effect. The MOFC is known to play a key role in the representation process of labelling the stimuli as self-referential, and the precuneus is known to be in charge of the integration process by linking the stimuli to a personal context (Northoff and Bermpohl, 2004). Thus, the stimuli is assumed to first be represented and labelled as self-referential by the MOFC and then further processed and integrated with self-context in the precuneus. We hence suggest that aberrant communication between these regions can cause "over-personalizing" of any given stimuli and thus intensify the focus on one's self-criticism. However, this needs to be further validated with a specific task that actively induce self-criticism.

Furthermore, accumulative evidence suggests that the DMN is highly involved in self-referential and specifically in ruminative processes. These studies, however, have been a priori examining specifically the DMN by either using the PCC/precuneus as a seed region (Cooney et al., 2010; Hamilton et al., 2011; Berman et al., 2011) or using the DMN reflective ICA component (Dutta et al., 2019; Zhu et al., 2012; Greicius et al., 2007). Here we show that data-driven whole-brain network approach was able to depict a significant correlation between DMN regions (precuneus and MOFC) and maladaptive rumination scores among depressed people. In addition, as opposed to earlier assumptions that maladaptive rumination in depression involves excessive DMN activity, further specific investigation of the intrinsic DMN connectivity we found that among high ruminators the DMN was overall less connected or "integrated" according to the network entropy measure. This result is in agreement with Mulders et al. (2015) review that indicate there is consistent findings showing changed connectivity between the anterior and posterior parts of the DMN. Our result is also in line with a recent large scale resting-state dataset, consisting of 1300 MDD patients, showing an overall reduction of DMN functional connectivity in patients with recurrent MDD compared to HC, which appears to be attributed by medication usage (Yan et al., 2019). Here, we found reduced DMN connectivity in relation to rumination scores both in patients, which most have been receiving medication treatment in the past, and HC whom never got any medication treatment. Moreover, the correlation between DMN entropy and rumination scores remained after controlling for medication usage within the MDD group (see Appendix 1).

Lastly, while ruminative thinking has been shown to be maladaptive among MDD patients, recent studies suggest that not all components of rumination are necessarily destructive (Treynor et al., 2003). Thus, the RRS questionnaire items can be sub-scaled into items with content overlap with depression labeled as "depression-related", anxious and gloomy thinking labeled as "brooding", and contemplation and pondering labeled as "self-reflection". While brooding and depression-related are maladaptive and are associated with a greater negative bias (Joormann and Gotlib, 2006), the self-reflection component can be considered as adaptive. Several studies had indicated that brooding and self-reflection ruminative scores have distinct neural signatures. For example, Hamilton et al. (2011) reported that dominance of the DMN over the task positive network was associated with higher levels of depression-related scores and lower levels of self-reflection rumination. Further exploration of our findings in relation to the three rumination subscales indicated that the effects were mostly driven by the depression-related and brooding components (see results Appendix 1). However, the self-reflection component did not exhibit a distinct pattern. These results can be explained by the high correlation between all three subscales within our cohort. In addition, Treynor et al. (2003) had shown that self-reflection is associated with concurrently more depression symptoms, however, less depression symptoms over time in a longitudinal study. Therefore, we suggest that our results indicate a more general rumination related mechanism that is also related to the current depression symptoms among MDD.

Several limitations of this study should be taken into account. First, in this study, we did not directly induce rumination among participant and there was no direct measure for rumination during the scan. Our results, therefore, implicate only on the functional brain network topology and hierarchy during rest as predictive of individual rumination trait and not of the rumination experience itself. Future studies should investigate if these network features and influences also dynamically change in relation to induced controlled rumination experience. Furthermore, future studies should include additional clinical measures relevant to rumination such as cognitive inflexibility and self-focused attention which could potentially enrich and expand our understanding of these results. It would also be of great interest to further conduct a longitudinal study design to test rather these network features could potentially predict relapse among remitted patients. Second, $D_{EP}NA$ can be used to make inferences regarding the influence hierarchy within a network, however, it does not infer a causal influence in the true sense, since correlation does not imply causation (Friston, 2009). We thus propose that the $D_{EP}NA$ results may target the crucial regions to define the specific model of connectivity required for causality testing methods such as the dynamic causal modeling (DCM) (Friston et al., 2003). Our results thus indicate that further studies using DCM should test the causality between the MOFC and precuneus.

To conclude, our findings emphasize the general DMN involvement in rumination pathophysiology among MDD. We add to existing research by inspecting the whole-brain network hierarchy and revealing the precuneus as a critical node and more specifically the impact of the MOFC on the precuneus as predictive of maladaptive rumination levels. In addition, compared to previous studies, this study was conducted on ultra-high field 7 T dataset which offers considerable advantage of improved quality of signal and thus allows for more precise functional connectivity analysis. In accordance with the RDoC new approach to study mental disorders, the significance of delineating basic psychological processes such as rumination in major depressive disorder and their dysfunction may advance our understanding regarding the underlying mechanisms of depression and its relevance to potential treatments. Future studies to expand this type of investigation should investigate rumination across different pathological populations such as different anxiety disorders obsessive compulsive disorder (OCD) or addiction.

CRediT authorship contribution statement

Yael Jacob: Conceptualization, Methodology, Software, Formal analysis, Writing - original draft, Visualization. **Laurel S Morris:** Conceptualization, Writing - review & editing. **Kuang-Han Huang:** Software. **Molly Schneider:** Investigation, Project administration. **Sarah Rutter:** Resources. **Gaurav Verma:** Investigation. **James W Murrough:** Supervision, Funding acquisition, Writing - review & editing. **Priti Balchandani:** Supervision, Funding acquisition, Writing - review & editing.

Declaration of Competing Interest

Dr. Priti Balchandani is a named inventor on patents relating to magnetic resonance imaging (MRI) and RF pulse design. The patents have been licensed to GE Healthcare, Siemens AG, and Philips international. Dr. Balchandani receives royalty payments relating to these patents. In the past 5 years, Dr. Murrough has provided consultation

services to Otsuka, Clexio Biosciences, Boehreinger Ingelheim, Sage Therapeutics, FSV7, Novartis, Allergan, Fortress Biotech, Janssen Research and Development, and Global Medical Education (GME) and has received research support from Avanir Pharmaceuticals, Inc. No other authors reported biomedical financial interests or potential conflicts of interest. However, there is no conflict of interest with respect to the content of this paper.

Acknowledgments

Funding was provided by NIH R01 MH109544. Additional support was provided by the Icahn School of Medicine Capital Campaign, Translational and Molecular Imaging Institute and Department of Radiology, Icahn School of Medicine at Mount Sinai and Siemens Healthcare.

Supplementary materials

Supplementary material associated with this article can be found, in the online version, at doi:10.1016/j.nicl.2019.102142.

References

Alkire, MT, Hudetz, AG, Tononi, G, 2008. Consciousness and anesthesia. Science 322 (5903), 876–880.
Alter, O., Brown, P.O., Botstein, D., 2000. Singular value decomposition for genome-wide expression data processing and modeling. Proc. Natl. Acad. Sci. 97, 10101–10106.
Andersson, J.L., Onoe, H., Hetta, J., Lidström, K., Valind, S., Lilja, A., et al., 1998. Brain networks affected by synchronized sleep visualized by positron emission tomography. J. Cereb. Blood Flow Metab. 18 (7), 701–715.
Bassett, D.S., Bullmore, E., Verchinski, B.A., Mattay, V.S., Weinberger, D.R., Meyer-Lindenberg, A., 2008. Hierarchical organization of human cortical networks in health and schizophrenia. J. Neurosci. 28 (37), 9239–9248.
Benjamini, Y., Hochberg, Y., 1995. Controlling the false discovery rate: a practical and powerful approach to multiple testing. J. R. Stat. Soc. Ser. B 57 (1), 289–300.
Berman, M.G., Peltier, S., Nee, D.E., Kross, E., Deldin, P.J., Jonides, J., 2011. Depression, rumination and the default network. Soc. Cognit. Affect. Neurosci. 6 (5), 548–555.
Bullmore, E., Sporns, O., 2009. Complex brain networks: graph theoretical analysis of structural and functional systems. Nat. Rev. Neurosci. 10 (3), 186–198.
Bullmore, E., Sporns, O., 2009. Complex brain networks: graph theoretical analysis of structural and functional systems. Nat. Rev. Neurosci. 10 (3), 186.
Cavanna, AE, Trimble, MR., 2006. The precuneus: a review of its functional anatomy and behavioural correlates. Brain 129 (3), 564–583.
Cavanna, AE., 2007. The precuneus and consciousness. CNS Spectrums 12 (7), 545–552.
Cooney, R.E., Joormann, J., Eugène, F., Dennis, E.L., Gotlib, I.H., 2010. Neural correlates of rumination in depression. Cognit. Affect. Behav. Neurosci. 10 (4), 470–478.
Cox, R.W.A.F.N.I., 1996. software for analysis and visualization of functional magnetic resonance neuroimages. Comput. Biomed. Res. Int. J. 29 (3), 162–173.
Desikan, RS, Segonne, F, Fischl, B, Quinn, BT, Dickerson, BC, Blacker, D, et al., 2006. An automated labeling system for subdividing the human cerebral cortex on MRI scans into gyral based regions of interest. NeuroImage 31 (3), 968–980.
Dutta, A., McKie, S., Downey, D., Thomas, E., Juhasz, G., Arnone, D., et al., 2019. Regional default mode network connectivity in major depressive disorder: modulation by acute intravenous citalopram. Transl. Psychiatry 9 (1), 116.
First, M, Williams, J, Karg, R, Spitzer, R, 2015. Structured Clinical Interview for DSM-5—Research version (SCID-5 for DSM-5, Research Version; SCID-5-RV). American Psychiatric Association, Arlington, VA.
Fossati, P., Hevenor, S.J., Graham, S.J., Grady, C., Keightley, M.L., Craik, F., et al., 2003. In search of the emotional self: an fMRI study using positive and negative emotional words. Am. J. Psychiatry 160 (11), 1938–1945.
Fox, M.D., Snyder, A.Z., Vincent, J.L., Corbetta, M., Van Essen, D.C., Raichle, M.E., 2005. The human brain is intrinsically organized into dynamic, anticorrelated functional networks. Proc. Natl. Acad. Sci. 102 (27), 9673–9678.
Friston, K., 2009. Causal modelling and brain connectivity in functional magnetic resonance imaging. PLoS Biol. 7 (2), e1000033.
Friston, KJ, Harrison, L, Penny, W, 2003. Dynamic causal modelling. NeuroImage 19 (4), 1273–1302.
Gelman, A, Hill, J, 2006. Data Analysis Using Regression and Multilevel/Hierarchical Models. Cambridge university press.
Goebel, R., Roebroeck, A., Kim, D.-S., Formisano, E., 2003. Investigating directed cortical interactions in time-resolved fMRI data using vector autoregressive modeling and Granger causality mapping. Magn. Reson. Imaging 21 (10), 1251–1261.
Gong, Q., He, Y., 2015. Depression neuroimaging and connectomics: a selective overview. Biol. Psychiatry 77 (3), 223–235.
Gong, G., He, Y., Concha, L., Lebel, C., Gross, D.W., Evans, A.C., et al., 2008. Mapping anatomical connectivity patterns of human cerebral cortex using in vivo diffusion tensor imaging tractography. Cereb. Cortex 19 (3), 524–536.
Greicius, M.D., Flores, B.H., Menon, V., Glover, G.H., Solvason, H.B., Kenna, H., et al., 2007. Resting-state functional connectivity in major depression: abnormally increased contributions from subgenual cingulate cortex and thalamus. Biol. Psychiatry 62 (5), 429–437.
Greicius, M.D., Krasnow, B., Reiss, A.L., Menon, V., 2003. Functional connectivity in the resting brain: a network analysis of the default mode hypothesis. Proc. Natl. Acad. Sci. 100 (1), 253–258.
Gusnard, D.A., Akbudak, E., Shulman, G.L., Raichle, M.E., 2001. Medial prefrontal cortex and self-referential mental activity: relation to a default mode of brain function. Proc. Natl. Acad. Sci. 98 (7), 4259–4264.
Gusnard, D.A., Akbudak, E., Shulman, G.L., Raichle, M.E., 2001. Medial prefrontal cortex and self-referential mental activity: relation to a default mode of brain function. Proc. Natl. Acad. Sci. USA 98 (7), 4259–4264.
Hagmann, P., Cammoun, L., Gigandet, X., Meuli, R., Honey, C.J., Wedeen, V.J., et al., 2008. Mapping the structural core of human cerebral cortex. PLoS Biol. 6 (7), e159.
Hamilton, J.P., Furman, D.J., Chang, C., Thomason, M.E., Dennis, E., Gotlib, I.H., 2011. Default-mode and task-positive network activity in major depressive disorder: implications for adaptive and maladaptive rumination. Biol. Psychiatry 70 (4), 327–333.
Iturria-Medina, Y, Sotero, RC, Canales-Rodríguez, EJ, Alemán-Gómez, Y, Melie-García, L, 2008. Studying the human brain anatomical network via diffusion-weighted MRI and graph theory. NeuroImage 40 (3), 1064–1076.
Jacob, Y., Gilam, G., Lin, T., Raz, G., Hendler, T., 2018a. Anger modulates influence hierarchies within and between emotional reactivity and regulation networks. Front. Behav. Neurosci. 12 (60).
Jacob, Y, Or-Borichev, A, Jackont, G, Lubianiker, N, Hendler, T, 2018b. Network Based fMRI Neuro-Feedback for Emotion Regulation; Proof-of-Concept. Springer International Publishing, Cham.
Jacob, Y, Papo, D, Hendler, T, Ben-Jacob, E, 2012. Functional holography and cliques in brain activation patterns. editor In: Chaudhary, DV (Ed.), Advances in Brain Imaging. InTech.
Jacob, Y., Rapson, A., Kafri, M., Baruchi, I., Hendler, T., Ben Jacob, E., 2010. Revealing voxel correlation cliques by functional holography analysis of fMRI. J. Neurosci. Methods 191 (1), 126–137.
Jacob, Y., Rosenberg-Katz, K., Gurevich, T., Helmich, R.C., Bloem, B.R., Orr-Urtreger, A., et al., 2019. Network abnormalities among non-manifesting Parkinson disease related LRRK2 mutation carriers. Hum. Brain Mapp.
Jacob, Y., Shany, O., Goldin, P.R., Gross, J.J., Hendler, T., 2018c. Reappraisal of interpersonal criticism in social anxiety disorder: a brain network hierarchy perspective. Cereb. Cortex bhy181-bhy.
Jacob, Y., Winetraub, Y., Raz, G., Ben-Simon, E., Okon-Singer, H., Rosenberg-Katz, K., et al., 2016. Dependency Network Analysis (DEPNA) reveals context related influence of brain network nodes. Sci. Rep. 6, 27444.
Joormann, J., Gotlib, I.H., 2006. Is this happiness I see? Biases in the identification of emotional facial expressions in depression and social phobia. J. Abnorm. Psychol. 115 (4), 705.
Kabbara, A., El Falou, W., Khalil, M., Wendling, F., Hassan, M., 2017. The dynamic functional core network of the human brain at rest. Sci. Rep. 7 (1), 2936.
Kawasaki, H., Adolphs, R., Kaufman, O., Damasio, H., Damasio, A.R., Granner, M., et al., 2001. Single-neuron responses to emotional visual stimuli recorded in human ventral prefrontal cortex. Nat. Neurosci. 4 (1), 15.
Kjaer, T., Nowak, M., Kjær, K.W., Lou, A., Lou, H., 2001. Precuneus–prefrontal activity during awareness of visual verbal stimuli. Conscious. Cognit. 10 (3), 356–365.
Korgaonkar, M.S., Fornito, A., Williams, L.M., Grieve, S.M., 2014. Abnormal structural networks characterize major depressive disorder: a connectome analysis. Biol. Psychiatry 76 (7), 567–574.
Kundu, P, Inati, SJ, Evans, JW, Luh, WM, Bandettini, PA, 2012. Differentiating BOLD and non-BOLD signals in fMRI time series using multi-echo EPI. NeuroImage 60 (3), 1759–1770.
Kundu, P, Inati, SJ, Evans, JW, Luh, W-M, Bandettini, PA, 2012. Differentiating BOLD and non-BOLD signals in fMRI time series using multi-echo EPI. NeuroImage 60 (3), 1759–1770.
Kundu, P, Voon, V, Balchandani, P, Lombardo, MV, Poser, BA, Bandettini, PA, 2017. Multi-echo fMRI: a review of applications in fMRI denoising and analysis of BOLD signals. NeuroImage 154, 59–80.
Maquet, P., Degueldre, C., Delfiore, G., Aerts, J., Péters, J.-M., Luxen, A., et al., 1997. Functional neuroanatomy of human slow wave sleep. J. Neurosci. 17 (8), 2807–2812.
Marques, JP, Kober, T, Krueger, G, van der Zwaag, W, Van de Moortele, P-F, Gruetter, R, 2010. MP2RAGE, a self bias-field corrected sequence for improved segmentation and T1-mapping at high field. NeuroImage 49 (2), 1271–1281.
Mars, R.B., Neubert, F.-X., Noonan, M.P., Sallet, J., Toni, I., Rushworth, M.F., 2012. On the relationship between the “default mode network” and the “social brain”. Front. Hum. Neurosci. 6, 189.
Montgomery, S.A., Asberg, M., 1979. A new depression scale designed to be sensitive to change. Br. J. Psychiatry 134, 382–389.
Morris, L.S., Kundu, P., Costi, S., Collins, A., Schneider, M., Verma, G., et al., 2019. Ultra-high field MRI reveals mood-related circuit disturbances in depression: a comparison between 3-Tesla and 7-Tesla. Transl. Psychiatry 9 (1), 94.
Mulders, P.C., van Eijndhoven, P.F., Schene, A.H., Beckmann, C.F., Tendolkar, I., 2015. Resting-state functional connectivity in major depressive disorder: a review. Neurosci. Biobehav. Rev. 56, 330–344.
Murrough, J.W., Abdallah, C.G., Anticevic, A., Collins, K.A., Geha, P., Averill, L.A., et al., 2016. Reduced global functional connectivity of the medial prefrontal cortex in major depressive disorder. Hum. Brain Mapp. 37 (9), 3214–3223.
Nejad, A., Fossati, P., Lemogne, C., 2013. Self-referential processing, rumination, and cortical midline structures in major depression. Front. Hum. Neurosci. 7 (666).
Nolen-Hoeksema, S., Morrow, J., Fredrickson, B.L., 1993. Response styles and the duration of episodes of depressed mood. J. Abnorm. Psychol. 102 (1), 20–28.

Nolen-Hoeksema, S., Wisco, B.E., Lyubomirsky, S., 2008. Rethinking rumination. Perspect. Psychol. Sci. 3 (5), 400–424.
Northoff, G., Bermpohl, F., 2004. Cortical midline structures and the self. Trends Cognit. Sci. 8 (3), 102–107.
Northoff, G., Heinzel, A., de Greck, M., Bermpohl, F., Dobrowolny, H., Panksepp, J., 2006. Self-referential processing in our brain – a meta-analysis of imaging studies on the self. NeuroImage 31 (1), 440–457.
Ochsner, K.N., Gross, J.J., 2005. The cognitive control of emotion. Trends Cognit. Sci. 9 (5), 242–249.
Philippi, C.L., Tranel, D., Duff, M., Rudrauf, D., 2014. Damage to the default mode network disrupts autobiographical memory retrieval. Soc. Cognit. Affect. Neurosci. 10 (3), 318–326.
Qin, P, Northoff, G., 2011. How is our self related to midline regions and the default-mode network? NeuroImage 57 (3), 1221–1233.
Raichle, M.E., MacLeod, A.M., Snyder, A.Z., Powers, W.J., Gusnard, D.A., Shulman, G.L., 2001. A default mode of brain function. Proc. Natl. Acad. Sci. USA 98 (2), 676–682.
Raichle, M.E., 2010. Two views of brain function. Trends Cognit. Sci. 14 (4), 180–190.
Rainville, P., Hofbauer, R.K., Paus, T., Duncan, G.H., Bushnell, M.C., Price, D.D., 1999. Cerebral mechanisms of hypnotic induction and suggestion. J. Cognit. Neurosci. 11 (1), 110–125.
Roberts, J.E., Gilboa, E., Gotlib, I.H., 1998. Ruminative response style and vulnerability to episodes of dysphoria: gender, neuroticism, and episode duration. Cognit. Ther. Res. 22 (4), 401–423.
Rubinov, M, Sporns, O., 2010. Complex network measures of brain connectivity: uses and interpretations. NeuroImage 52 (3), 1059–1069.
Sanislow, C.A., Pine, D.S., Quinn, K.J., Kozak, M.J., Garvey, M.A., Heinssen, R.K., et al., 2010. Developing constructs for psychopathology research: research domain criteria. J. Abnorm. Psychol. 119 (4), 631–639.
Schilbach, L., Eickhoff, S.B., Rotarska-Jagiela, A., Fink, G.R., Vogeley, K., 2008. Minds at rest? Social cognition as the default mode of cognizing and its putative relationship to the “default system” of the brain. Conscious. Cognit. 17 (2), 457–467.
Shannon, CE., 1949. A mathematical theory of communication (Part I). BSTJ 27, 379–423.
Shapira, Y., Kenett, D.Y., Ben-Jacob, E., 2009. The index cohesive effect on stock market correlations. Eur. Phys. J. B 72 (4), 657.
Sheline, Y.I., Barch, D.M., Price, J.L., Rundle, M.M., Vaishnavi, S.N., Snyder, A.Z., et al., 2009. The default mode network and self-referential processes in depression. Proc. Natl. Acad. Sci. 106 (6), 1942–1947.
Sporns, O., 2010. Networks of the Brain. MIT press.
Spreng, R.N., Mar, R.A., Kim, A.S., 2009. The common neural basis of autobiographical memory, prospection, navigation, theory of mind, and the default mode: a quantitative meta-analysis. J. Cognit. Neurosci. 21 (3), 489–510.
Treynor, W., Gonzalez, R., Nolen-Hoeksema, S., 2003. Rumination reconsidered: a psychometric analysis. Cognit. Ther. Res. 27 (3), 247–259.
van der Meer, L., Costafreda, S., Aleman, A., David, A.S., 2010. Self-reflection and the brain: a theoretical review and meta-analysis of neuroimaging studies with implications for schizophrenia. Neurosci. Biobehav. Rev. 34 (6), 935–946.
Varshavsky, R, Gottlieb, A, Horn, D, Linial, M, 2007. Unsupervised feature selection under perturbations: meeting the challenges of biological data. Bioinformatics 23 (24), 3343–3349.
Yan, C.-G., Chen, X., Li, L., Castellanos, F.X., Bai, T.-J., Bo, Q.-J., et al., 2019. Reduced default mode network functional connectivity in patients with recurrent major depressive disorder. Proc. Natl. Acad. Sci. 116 (18), 9078–9083.
Zhang, J., Wang, J., Wu, Q., Kuang, W., Huang, X., He, Y., et al., 2011. Disrupted brain connectivity networks in drug-naive, first-episode major depressive disorder. Biol. Psychiatry 70 (4), 334–342.
Zhu, X., Wang, X., Xiao, J., Liao, J., Zhong, M., Wang, W., et al., 2012. Evidence of a dissociation pattern in resting-state default mode network connectivity in first-episode, treatment-naive major depression patients. Biol. Psychiatry 71 (7), 611–617.